Gazi Üniversitesi
Fen Bilimleri Dergisi
PART C: TASARIM VE TEKNOLOJİ

Gazi University
Journal of Science
PART C: DESIGN AND TECHNOLOGY

GU J Sci, Part C, 11(4): 1232-1243 (2023)

A Comparison of Digital Constant On-Time and Variable On-Time Control in Buck/Buck-Boost PFC Converter

Zafer ORTATEPE[1*]

[1]Pamukkale University, The Department of Automotive Engineering, Denizli, Turkey

Article Info

Research article
Received:15/06/2023
Revision:19/09/2023
Accepted:16/10/2023

Keywords

Buck/buck-boost converter Constant on-time control Variable on-time control

Makale Bilgisi

Araştırma makalesi
Başvuru:15/06/2023
Düzeltme:19/09/2023
Kabul:16/10/2023

Anahtar Kelimeler

Buck/buck-boost dönüştürücü
Sabit açık zaman kontrol
Değişken açık zaman kontrol

Graphical Abstract (Grafik Özet)

This study compares constant on-time (COT) and variable on-time (VOT) control techniques for completely digitally controlled buck/buck-boost power factor correction (PFC) converters operated in critical conduction mode (CRM). It examines the dynamic behavior of converters under various operating conditions to better understand the stability and robustness of the control system. / Bu çalışma, kritik iletim modunda (CRM) çalıştırılan tamamen dijital olarak kontrol edilen düşürücü/düşürücü-yükseltici güç faktörü düzeltme (PFC) dönüştürücüleri için sabit açık zaman (COT) ve değişken açık zaman (VOT) kontrol tekniklerini karşılaştırır. Kontrol sisteminin kararlılığını ve sağlamlığını daha iyi anlamak için dönüştürücülerin çeşitli çalışma koşulları altındaki dinamik davranışını inceler.

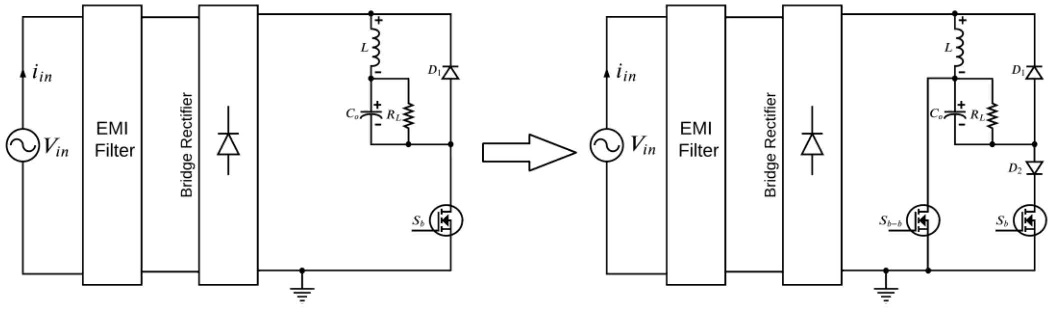

***Figure A**: Conventional buck PFC and buck/buck-boost PFC converter /**Şekil A:**.Klasik düşürücü PFC ve düşürücü/düşürücü-yükseltici PFC döünüştürücü*

Highlights (Önemli noktalar)

- *The paper allows fully digitally controlled COT and VOT control methods to be applied to the buck/buck-boost converter. / Makale, tamamen dijital olarak kontrol edilen COT ve VOT kontrol yöntemlerinin düşürücü/düşürücü-yükseltici dönüştürücüye uygulanmasına olanak tanır.*
- *The THD and PF values obtained from both control methods under different load and input voltage conditions are compared. / Her iki kontrol yönteminin farklı yük ve giriş gerilimi koşulları altında elde edilen THD ve PF değerleri karşılaştırılır.*
- *By presenting simulation results, an important gap in the literature has been eliminated. / Simülasyon sonuçları sunularak literatürdeki önemli bir eksiklik giderilmiştir.*

Aim (Amaç): *The aim is to apply fully digital control methods to the buck/buck-boost PFC converter and compare the total harmonic distortion (THD) and power factor (PF) performances of these control strategies. / Amaç, düşürücü/düşürücü-yükseltici PFC dönüştürücüye tamamen dijital kontrol yöntemlerini uygulamak ve bu kontrol stratejilerinin toplam harmonik bozulma (THD) ve güç faktörü (PF) performanslarını karşılaştırmaktır.*

Originality (Özgünlük): *A significant weakness in the literature on this topic is the lack of simulations in the papers. The absolutely separates this study from other studies in the literature is the thorough reporting of the completely digital controlled converter simulation results. / Bu konuyla ilgili literatürdeki önemli bir zayıflık, makalelerde simülasyonların bulunmamasıdır. Bu çalışmayı literatürdeki diğer çalışmalardan kesinlikle ayıran şey, tamamen dijital kontrollü dönüştürücü simülasyon sonuçlarının kapsamlı bir şekilde raporlanmasıdır.*

Results (Bulgular): *The VOT control method demonstrates higher PF and lower THD compared to the COT control method for both 220V_{AC} and 110V_{AC} input voltage under full load conditions. / VOT kontrol yöntemi, tam yük koşulları altında hem 220V_{AC} hem de 110V_{AC} giriş voltajı için COT kontrol yöntemiyle karşılaştırıldığında daha yüksek PF ve daha düşük THD gösterir.*

Conclusion (Sonuç): *The VOT control strategy offers the advantage over COT of dynamically adapting the on-time based on input and output voltage conditions, resulting in improved load regulation and stability. / VOT kontrol stratejisi, giriş ve çıkış voltajı koşullarına dayalı olarak açık kalma süresini dinamik olarak uyarlama konusunda COT'ye göre avantaj sunar ve bu da gelişmiş yük düzenlemesi ve stabilite sağlar.*

*Corresponding author, e-mail: zortatepe@pau.edu.tr

DOI: 10.29109/gujsc.1314903

GU J Sci, Part C, 11(4): 1232-1243 (2023)

Gazi Üniversitesi
Fen Bilimleri Dergisi
PART C: TASARIM VE TEKNOLOJİ

Gazi University
Journal of Science
PART C: DESIGN AND TECHNOLOGY

http://dergipark.gov.tr/gujsc

A Comparison of Digital Constant On-Time and Variable On-Time Control in Buck/Buck-Boost PFC Converter

Zafer ORTATEPE[1*]

[1]*Pamukkale University, The Department of Automotive Engineering, Denizli, Turkey*

Article Info

Research article
Received:15/06/2023
Revision:19/09/2023
Accepted:16/10/2023

Keywords

Buck/buck-boost converter
Constant on-time control
Variable on-time control

Abstract

This paper compares two frequently used control strategies for fully digitally controlled buck/buck-boost power Factor Correction (PFC) converters operated in critical conduction mode (CRM): constant on-time (COT) and variable on-time (VOT). The aim is to evaluate and compare the total harmonic distortion (THD) and power factor (PF) performance of these control strategies. The COT control technique employs a fixed on-time period for each switching cycle, resulting in a predictable and straightforward control scheme. On the other hand, VOT control dynamically adapts the on-time period based on the input and output voltage conditions, offering potential advantages in terms of load regulation and stability. Results of the paper ensure precious insights into strengths and limitations of each control technique. Additionally, the dynamic behavior of the converters under various operating conditions is investigated, shedding light on the stability and robustness aspects of each control scheme. The study is conducted using a fully digital setup and evaluated in Matlab/Simulink software platform. The results demonstrate that under steady-state conditions, VOT control superior to COT in terms of THD and PF. These results provide valuable insight on selecting a suitable control method for PFC converters, considering specific requirements of their applications.

Buck/Buck-Boost PFC Dönüştürücüde Dijital Sabit Açık Zaman ve Değişken Açık Zaman Kontrolün Karşılaştırılması

Makale Bilgisi

Araştırma makalesi
Başvuru:15/06/2023
Düzeltme:19/09/2023
Kabul:16/10/2023

Anahtar Kelimeler

Buck/buck-boost dönüştürücü
Sabit açık zaman kontrol
Değişken açık zaman kontrol

Öz

Bu makale, kritik iletim modunda (CRM) çalıştırılan tamamen dijital olarak kontrol edilen düşürücü/düşürücü-yükseltici güç faktörü düzeltme (PFC) dönüştürücüleri için sıklıkla kullanılan iki kontrol stratejisini karşılaştırır: sabit açık zaman (VOT) ve değişken açık zaman (VOT). Amaç, bu kontrol stratejilerinin toplam harmonik bozulma (THD) ve güç faktörü (PF) performansını değerlendirmek ve karşılaştırmaktır. COT kontrol tekniği, her anahtarlama döngüsü için sabit bir açık kalma süresi kullanır ve bu da öngörülebilir ve basit bir kontrol şemasıyla sonuçlanır. Öte yandan VOT kontrolü, giriş ve çıkış voltajı koşullarına göre açık kalma süresini dinamik olarak uyarlayarak yük düzenlemesi ve kararlılık açısından potansiyel avantajlar sunar. Makalenin sonuçları, her kontrol tekniğinin güçlü yönleri ve sınırlamaları hakkında değerli bilgiler sağlamaktadır. Ek olarak, dönüştürücülerin çeşitli çalışma koşulları altındaki dinamik davranışları incelenerek her kontrol şemasının kararlılık ve sağlamlık yönlerine ışık tutulmuştur. Çalışma tamamen dijital ortamda gerçekleştirilmiş ve Matlab/Simulink yazılım platformunda değerlendirilmiştir. Sonuçlar, kararlı durum koşulları altında VOT kontrolünün, THD ve PF açısından COT'dan daha üstün olduğunu göstermektedir. Bu sonuçlar, uygulamalarının özel gereksinimleri dikkate alınarak PFC dönüştürücüler için uygun bir kontrol yönteminin seçilmesi konusunda değerli bilgiler sağlamaktadır.

1. INTRODUCTION (GİRİŞ)

AC/DC power conversion systems play a crucial role in various power electronic devices, enabling efficient power conversion from the AC grid to DC load. However, the increasing number of devices has given rise to a significant concern: harmonic pollution. In response, various power factor correction (PFC) circuits have been designed to comply with IEC 61000-3-2 current harmonic standards, effectively addressing this issue. These circuits aim to ensure high PF and low THD in power systems. Among different types of AC/DC PFC converters, boost, buck-boost, buck, cúk, and sepic converters are commonly used due to their

*Corresponding author, e-mail: zortatepe@pau.edu.tr
DOI: 10.29109/gujsc.1314903

versatility and wide range of applications. Each topology has unique benefits and drawbacks.

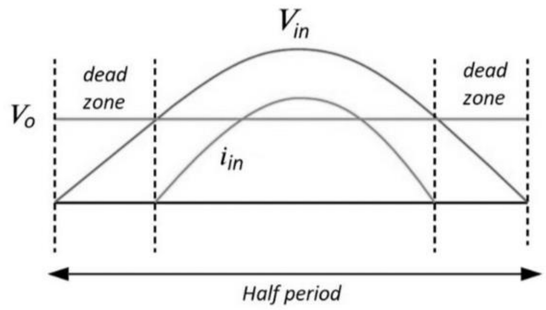

Figure 1. Current and voltage waveforms of the conventional buck PFC converter (Klasik düşürücü PFC devresinin akım ve gerilim dalga formları)

The boost PFC converter [1] increases voltage, helping to stabilize voltage and enhance power factor (PF), but it may also increase current stress on the switch due to continuous conduction mode (CCM) operation. The buck-boost PFC converter [2] combines the benefits of both boost and buck converters but requires careful design to mitigate switching losses. Also, even if the topology has a single switch, inversion of output leads to a complex sensing and feedback circuit. Cúk [3] and sepic [4] PFC converters are known for their ability to provide step-up/step-down capability of the output voltage and to reducing voltage stress on semiconductors, ideal for high-power applications. However, the main drawback of these topologies is that they have the same voltage gain as buck-boost converters but require more components. On the contrary, the buck PFC converter efficiently reduces voltage, improving voltage stress on the switches, voltage regulation, and conduction losses, making it suitable for applications where voltage reduction is required. Nevertheless, due to its dead zones, the conventional buck PFC converter is unable to control the input current to be fully sinusoidal, which results of significant losses in regions where the input voltage is lower than the output voltage. Consequently, the circuit has trouble meeting with the IEC61000-3-2 current harmonic limits. Figure 1 shows the input and output voltages as well as the input current waveforms for conventional buck PFC converter within a half period.

The implementation of the constant on-time (COT) control method to the buck PFC converter was first discussed in [5]. In this study, where dead zones could not be entirely eliminated, a power factor (PF) of 0.965 was achieved. First study in which variable on-time (VOT) control method is applied to the buck PFC converter is presented in [6]. However, the reported study was unable to eliminate dead zones. Another noteworthy study in which the COT control method and soft switching technique are used both to the buck converter is presented in [7]. The study on eliminating the dead zones of the buck PFC converter with additional circuit is given in [8]. The new topology obtained by adding a switch and two diodes is superior to the conventional ones. The implementation of the fully analog VOT control method to the flyback circuit is given in [9]. A study on the control of the buck PFC converter with the COT control method is also presented in [10]. However, dead zones could not be controlled. The study in which flyback topology is added to eliminate dead zones in the forward converter is presented in [11]. The forward PFC converter is similar to the buck PFC converter in that it has dead zones in regions where the input voltage is lower than the output voltage.

It is presented in the fully analog controlled buck PFC converter [12], where the switching frequency is reduced with the VOT control method. In addition, the study in which the improved VOT control technique is applied to a fully analog controlled CRM flyback PFC converter is given in [13]. The implementation of VOT control technique to buck-flyback PFC topology is explained in [14]. The application of the VOT control technique to a fully digitally controlled flyback topology is first presented in [15]. Fully analog VOT controlled buck/buck-boost PFC converter implementation is given in [16]. Segmented COT control method is applied to the buck/buck-boost PFC converter in [17]. Besides, fully analog constant switching frequency control method for the conventional buck/buck-boost PFC converter is applied in [18]. In [19], fixed on-time ratio control (FOTRC) and fixed duty-cycle ratio control (FDCRC) method have been implemented to the buck/buck-boost PFC converter. Finally, the buck PFC topology controlled by only single switch is given in [20]. In the literature, other than the COT and VOT control techniques, some papers based on soft switching techniques have also been presented to eliminate dead zones of the buck PFC converter [21], [22].

Analog control approach is proposed in almost all of the above-mentioned studies. Major gap in the literature regarding this topic is the lack of presentation of simulations in the papers. This paper presents a comparison for fully digital COT and VOT control methods and its implementation for buck/buck-boost PFC topology given in [16]. The complete reporting of simulation results of fully digital controlled converter in this study stands out as the most important aspect that separates it from other studies in the literature. The simulation is carried out in MATLAB/Simulink.

The rest of this paper is as follows: In section 2, operating principle of the buck/buck-boost converter is presented. Analysis and implementation of the COT and VOT control methods is presented in section 3. Results of the study are given in section 4. Finally, the conclusion section is presented.

2. OPERATING PRINCIPLE OF THE CRM BUCK/BUCK-BOOST CONVERTER

(DÜŞÜRÜCÜ/DÜŞÜRÜCÜ-YÜKSELTİCİ DÖNÜŞTÜRÜCÜNÜN ÇALIŞMA PRENSİBİ)

Figure 2 shows the main circuit of the buck/buck-boost converter topology. The topology consists of EMI filter, universal bridge rectifier, inductor (L), output capacitor (C_o), freewheeling diode (D_1), output load (R_L), buck (S_b) and buck-boost switches (S_{b-b}).

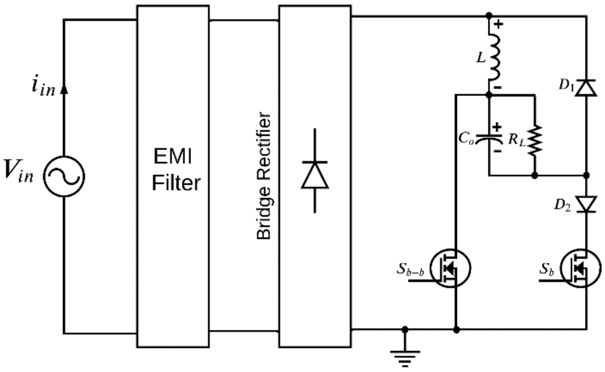

Figure 2. Main circuit of the buck/buck-boost converter topology ([16]) (Düşürücü/düşürücü-yükseltici topolojisinin ana devresi)

When input voltage is greater than output voltage, converter operates in buck mode; otherwise, it operates in buck-boost mode. Circuit is controlled in CRM and the steady state analysis can be implemented in two cases: $V_{in} > V_o$ and $V_{in} < V_o$.

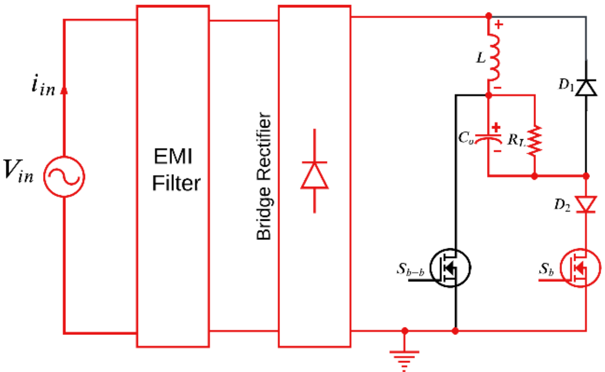

(a)

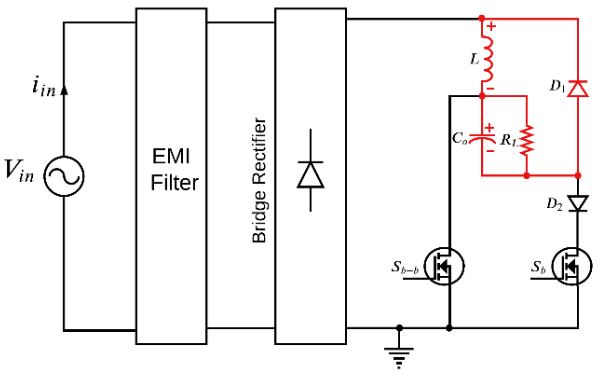

(b)

Figure 3. Operation modes of the topology in buck mode (a) S_b is turned-on (b) S_b is turned-off (Düşürücü modunda topolojinin çalışma modları (a) S_b açık (b) S_b kapalı)

When $V_{in} > V_o$, the topology operates in buck mode. S_b switch is active and S_{b-b} switch is in zero state, during this mode. Therefore, this mode has two states depending on the position of the S_b switch. These modes are given in Figure 3 (a) and (b), respectively. Besides, current shapes of the topology operated in CRM buck mode is shown in Figure 4.

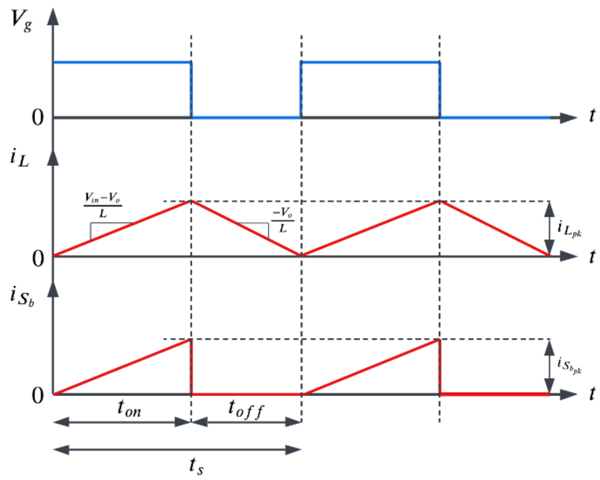

Figure 4. Current shapes of the topology operated in CRM buck mode (CRM düşürücü modda çalışan topolojinin akım biçimleri)

The detailed equations of the circuit operating in buck mode can be examined in [16]. During the buck mode, average input current of the converter is calculated as:

$$i_{in_{b\_avg}} = \frac{1}{2} i_{L_{pk_1}} D_b \quad (1)$$

$$i_{in_{b\_avg}} = \frac{V_o(V_{max}|sin\omega t| - V_o)t_{on}}{2LV_{max}|sin\omega t|} \quad (2)$$

where $i_{L_{pk_1}}$ is inductor current peak value, D_b is duty cycle ($D_b = t_{on}/t_s$), $V_{max}|sin\omega t|$ is sinusoidal input voltage, V_o is output voltage, L is inductor value and $i_{in_{b\_avg}}$ is average input current value of the converter in buck mode.

When $V_{in} < V_o$, the topology operates in buck-boost mode. S_{b-b} switch is active and S_b switch is in zero state during this mode. Therefore, this mode has two states depending on the position of the S_{b-b} switch. These modes are shown in Figure 5 (a) and (b), respectively. Besides, the current shapes of the buck/buck-boost converter topology operated in buck-boost mode is given in Figure 6.

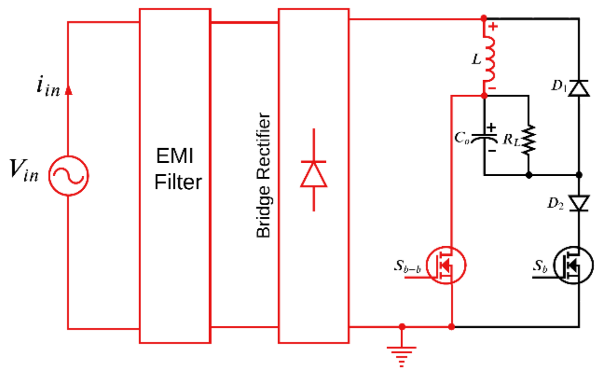

(a)

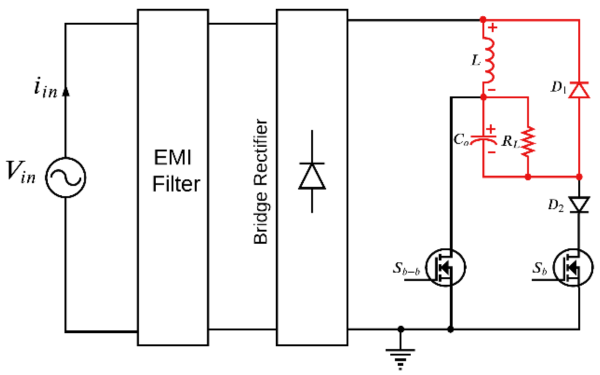

(b)

Figure 5. Operation modes of the topology in buck-boost mode (a) S_{b-b} is turned-on (b) S_{b-b} is turned-off (Düşürücü-yükseltici modunda topolojinin çalışma modları (a) S_{b-b} açık (b) S_{b-b} kapalı)

The detailed equations of the circuit operating in buck-boost mode are given in [16]. During the buck-boost mode, average input current of the converter is calculated as:

$$i_{in_{bavg}} = \frac{1}{2} i_{L_{pk_2}} D_{b-b} \tag{3}$$

$$i_{in_{b-bavg}} = \frac{V_o V_{max}|sin\omega t|}{2L(V_{max}|sin\omega t| + V_o)} t_{on} \tag{4}$$

where $i_{L_{pk_2}}$ is inductor current peak value, D_{b-b} is duty cycle ($D_{b-b} = t_{on}/t_s$) and $i_{in_{b-bavg}}$ is average input current value of the converter in buck-boost mode.

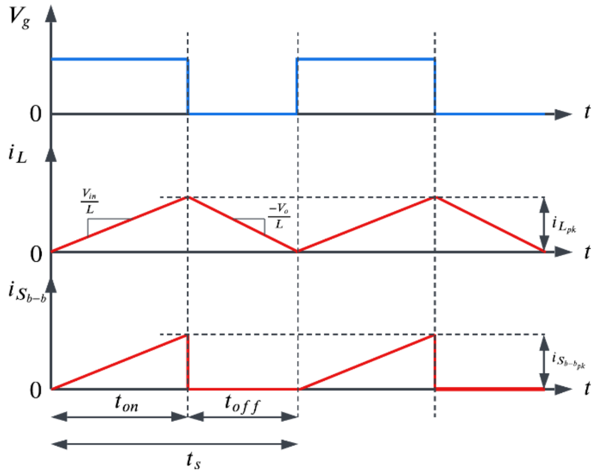

Figure 6. Current shapes of the topology operated in CRM buck-boost mode (CRM düşürücü-yükseltici modda çalışan topolojinin akım biçimleri)

3. IMPLEMENTATION OF DIGITAL COT CONTROL METHOD (COT KONTROL METODUNUN UYGULANMASI)

According to the analysis above, the average input current for the COT control is defined as follows:

$$i_{in_{COT}} = \begin{cases} \frac{t_{on}V_o}{2L}\left(\frac{V_{max}|sin\omega t| - V_o}{V_{max}|sin\omega t|}\right) \\ (\theta \le \omega t \le \pi - \theta) \\ \frac{t_{on}V_o}{2L}\left(\frac{V_{max}|sin\omega t|}{V_{max}|sin\omega t| + V_o}\right) \\ (0 \le \omega t \le \theta \ \& \ \pi - \theta < \omega t < \pi) \end{cases} \tag{5}$$

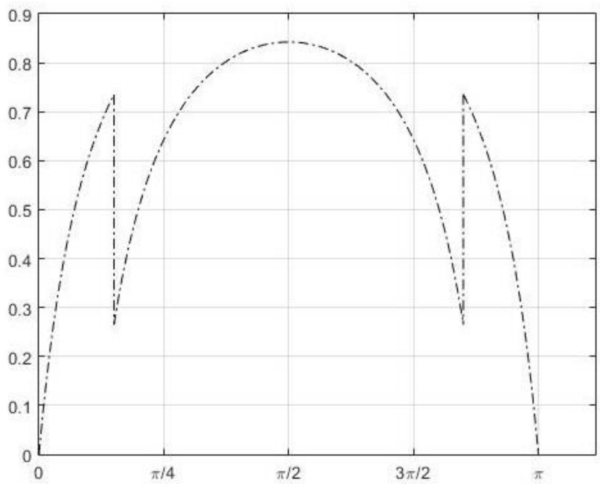

Figure 7. Average input current waveform of the COT controlled buck/buck-boost topology (COT kontrollü düşürücü/düşürücü-yükseltici topolojinin ortalama giriş akımı dalga formu)

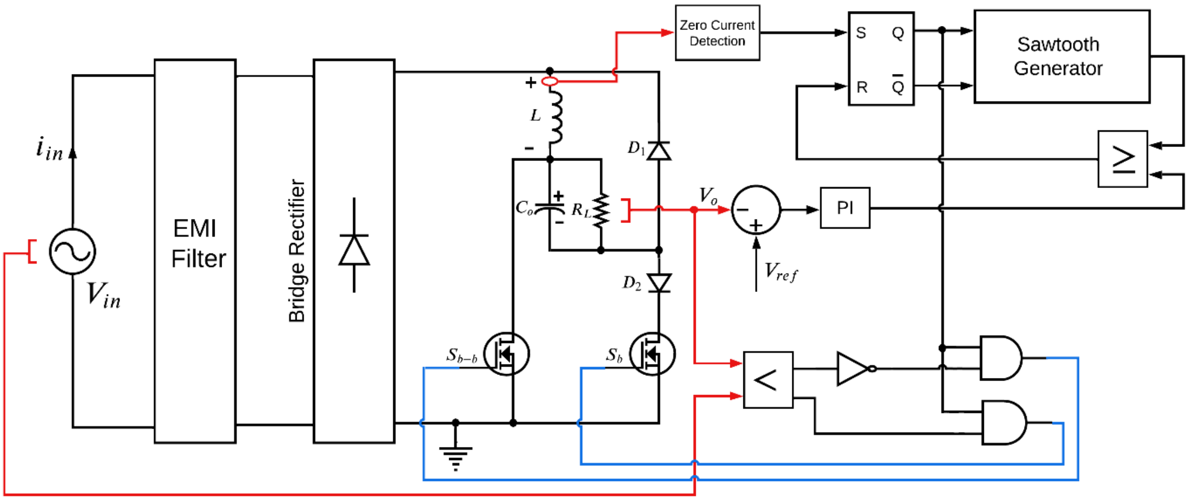

Figure 8. Control scheme for the digital COT controlled CRM buck/buck-boost topology (Dijital COT kontrollü CRM düşürücü/düşürücü-yükseltici topoloji için kontrol şeması)

While t_{on}, V_o, and L terms are constant in steady-state, terms in parentheses are not sinusoidal according to the equation (5). Hence, in the COT method, it is not possible for the average input current to be sinusoidal. Figure 7 shows average input current resulting from COT control for $220\sin(\omega t)$ input voltage, $80V_{DC}$ output voltage, 100W output power and $L = 118\mu H$ conditions.

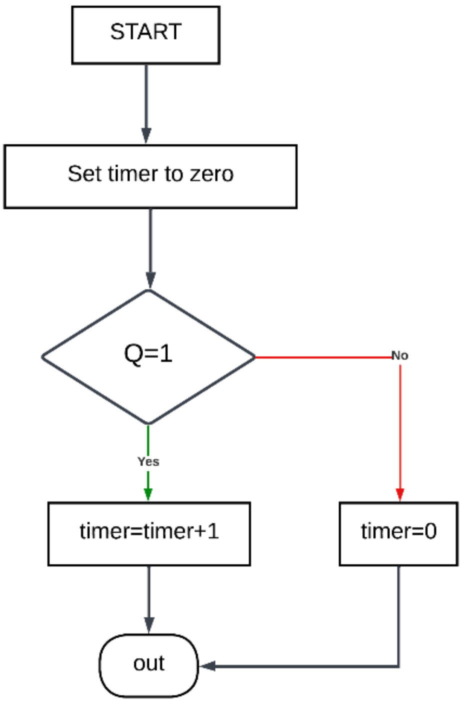

Figure 9. The flowchart of the sawtooth generator algorithm (Testere dişi jeneratör algoritması akış diyagramı)

The aim of this paper is not to give all mathematical equations, but to simplify the study and perform it in a digital environment. For detailed analysis of all equations, [16] can be examined. Digital control scheme for COT controlled buck/buck-boost topology is given in Figure 8. Zero current detection method is used for the detection zero points of inductor current. Gate signals of the switches are generated by SR flip-flop and a digital sawtooth generator block. This control scheme ensures variable switching frequency and forces to obtain sinusoidal input current.

In Figure 8, the digital component responsible for enabling the COT operation of the circuit is the sawtooth generator block. The flowchart of this block is provided in Figure 9. According to the flowchart, when the switch is on-state, the timer continuously counts; while when it is off-state the timer is reset. The data obtained at the output of this sawtooth generator block is compared with the data from the PI block as shown in Figure 8, leading to the resetting of the SR-type flip-flop.

4. IMPLEMENTATION OF DIGITAL VOT CONTROL METHOD (VOT KONTROL METODUNUN UYGULANMASI)

To provide unity PF in buck operation mode, t_{on} in equation (5) should be expressed as follows.

$$t_{on} = \frac{(V_{max}|\sin\omega t|)^2}{V_o(V_{max}|\sin\omega t| - V_o)} \quad (\theta \le \omega t \le \pi - \theta) \tag{6}$$

Therefore, average input current in buck mode is calculated as follows:

$$i_{in_{bavg}} = \frac{V_{max}|\sin\omega t|}{2L} \quad (\theta \le \omega t \le \pi - \theta) \tag{7}$$

Also, to provide unity PF in buck-boost operation mode as given in (5), t_{on} should be expressed as follows.

$$t_{on} = \frac{V_{max}|sin\omega t| + V_o}{V_o} \quad (0 \leq \omega t \leq \theta \ \& \ \pi - \theta < \omega t < \pi) \tag{8}$$

Hence, average input current in buck-boost mode is calculated given below:

$$i_{in_{b\_bavg}} = \frac{V_{max}|sin\omega t|}{2L} \quad (0 \leq \omega t \leq \theta \ \& \ \pi - \theta < \omega t < \pi) \tag{9}$$

As a result, in buck-boost mode, average input current of the topology is given below:

$$i_{in_{VOT}} = \begin{cases} \frac{V_{max}|sin\omega t|}{2L} & (\theta \leq \omega t \leq \pi - \theta) \\ \frac{V_{max}|sin\omega t|}{2L} & (0 \leq \omega t \leq \theta \ \& \ \pi - \theta < \omega t < \pi) \end{cases} \tag{10}$$

According to the equation (10), input current of the converter is pure sinusoidal for all conditions (buck and buck/buck-boost modes) and ensure high PF and low THD. Figure 10 shows average input current resulting from VOT control for $220\sin(\omega t)$ input voltage, $80V_{DC}$ output voltage, 100W output power and $L = 118\mu H$ conditions.

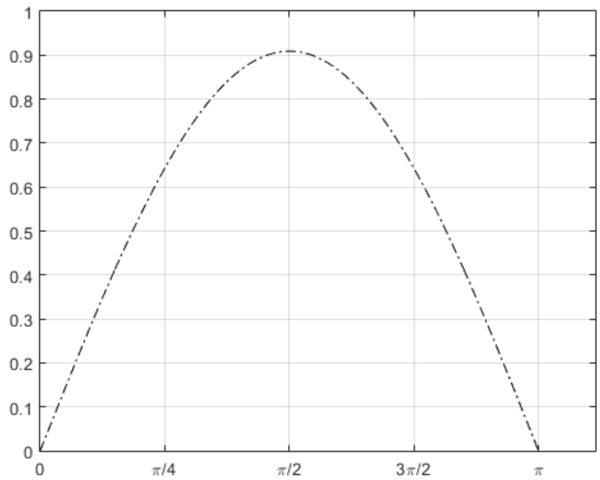

Figure 10. Average input current waveform of VOT controlled buck/buck-boost topology (VOT kontrollü düşürücü/düşürücü-yükseltici topolojinin ortalama giriş akımı dalga formu)

When the S_b switch is turned-on, the current across the current sense resistance can be expressed as follows:

$$v_{Rs_1} = \frac{V_{max}|sin\omega t| - V_o}{L} \, t_{on} \tag{11}$$

When equation (6) is applied to equation (11):

$$v_{Rs_1} = \frac{(V_{max}|sin\omega t|)^2}{V_o L} \tag{12}$$

In addition, when the S_{b-b} switch is turned-on, the current across the current sense resistance can be expressed as follows:

$$v_{Rs_2} = \frac{V_{max}|sin\omega t|}{L} \, t_{on} \tag{13}$$

When equation (8) is applied to equation (13):

$$v_{Rs_2} = \frac{(V_{max}|sin\omega t|)(V_{max}|sin\omega t| + V_o)}{V_o L} \tag{14}$$

The operating principle of the VOT control method is based on generating a reference inductor current and comparing the actual inductor current with this reference. The mathematical equation of the reference inductor current for buck mode is calculated as follows:

$$i_{L_{ref\_buck}} = \left(K_{p_1}\left(V_{ref} - V_o\right) + K_{i_1} \int \left(V_{ref} - V_o\right) dt\right) \left(\frac{(V_{max}|sin\omega t|)^2}{V_o L}\right) \tag{15}$$

where V_{ref} is reference output voltage, V_o is actual output voltage, K_{p_1} and K_{i_1} are proportional and integral terms of the PI controller. Besides, for the proportional and integral terms of PI controller $K_{p_1} = 0.1$ and $K_{i_1} = 7$ coefficients are used.

Also, the mathematical equation of the reference inductor current for buck mode is calculated as follows:

$$i_{L_{ref\_buck}} = \left(K_p\left(V_{ref} - V_o\right) + K_i \int \left(V_{ref} - V_o\right) dt\right) \left(\frac{(V_{max}|sin\omega t|)(V_{max}|sin\omega t| + V_o)}{V_o L}\right) \tag{16}$$

$K_{p_2} = 0.1$ and $K_{i_2} = 3$ coefficients are used for the PI controller's proportional and integral terms, respectively.

Digital control scheme for VOT controlled buck/buck-boost converter is shown in Figure 11. In this figure V_{in} represents $V_{max}|sin\omega t|$. Zero current detection method is used for the detection zero points of inductor current. Gate signals of the switches are generated by the SR flip-flop. This control scheme ensures variable switching frequency to provide pure sinusoidal input current. Although the VOT control method is more complex than the COT method, it gives better results in terms of sinusoidal input current, PF and THD.

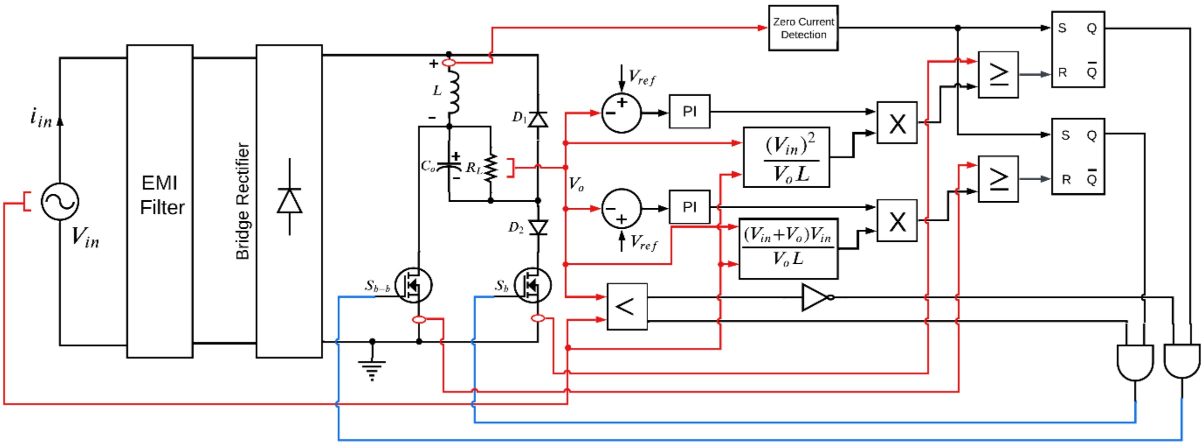

Figure 11. Control scheme for the digital VOT controlled CRM buck/buck-boost topology (Dijital VOT kontrollü CRM düşürücü/düşürücü-yükseltici topoloji için kontrol şeması)

5. SIMULATION RESULTS (SİMÜLASYON SONUÇLARI)

The simulation studies are carried out by the MATLAB/Simulink software platform to evaluate the performance of COT and VOT control methods under various parameter variation conditions. PF and THD values are obtained as the key metrics for comparison. Besides, the key variables used to carry out the simulation are listed in Table 1.

Table 1. The key variables used to carry out the simulation (Simülasyonu gerçekleştirmek için kullanılan temel değişkenler)

Parameters	Symbols	Values
Input voltage	V_{in}	90-270 [VAC]
Output load	R_L	64 [Ω]
Inductance	L	118 [µH]
Capacitor	C_o	1000 [µF]
Output power	P_o	100 [W]
Line frequency	f	50 [Hz]

A digital low pass filter is used for a non-filtered input current. Transfer function block in MATLAB/Simulink is used for the filter of input current and transfer function of this digital low pass filter is given below:

$$Filter_{TF} = \frac{1}{0.0003s+1} \tag{17}$$

Figure 12 (a) shows the control scheme of the digital COT controlled buck/buck-boost converter in MATLAB/Simulink. Besides, Figure 12 (b) shows the digital COT controller design. It can be seen from the figure that a separate sawtooth wave generator is used for both switching elements.

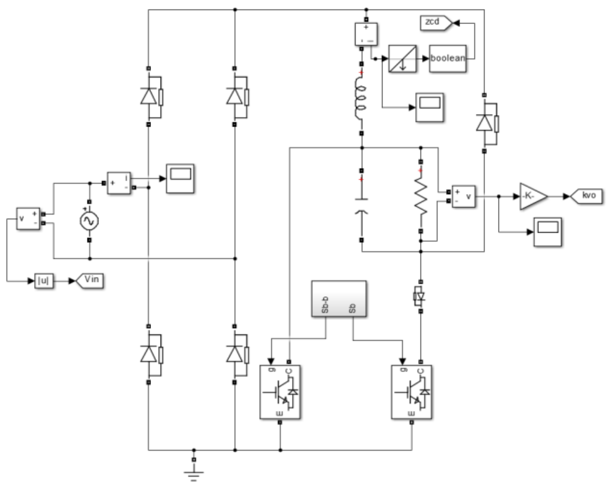

(a)

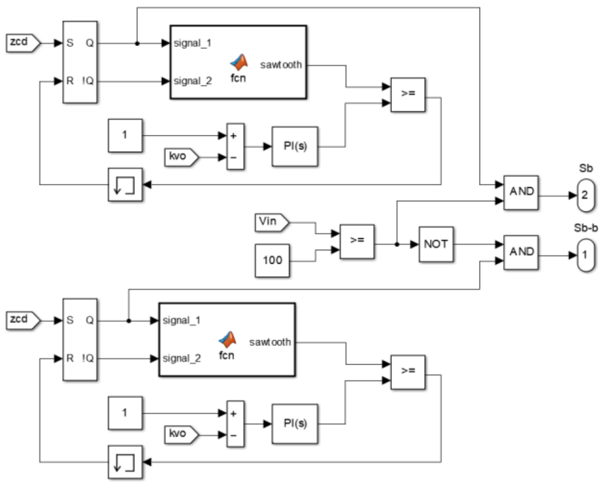

(b)

Figure 12. (a) Control scheme of the digital COT controlled converter (b) controller design ((a) Dijital

COT kontrollü dönüştürücünün kontrol şeması (b) kontrolör dizaynı)

Figure 13 (a) and (b) show the input current, inductor current, filtered input current and output voltage waveforms of the digital COT controlled buck/buck-boost converter for 220V_{AC} and 110 V_{AC} input voltage conditions, respectively. As can be seen from the figure, input current quality suffers as the input voltage decreases in the COT control method.

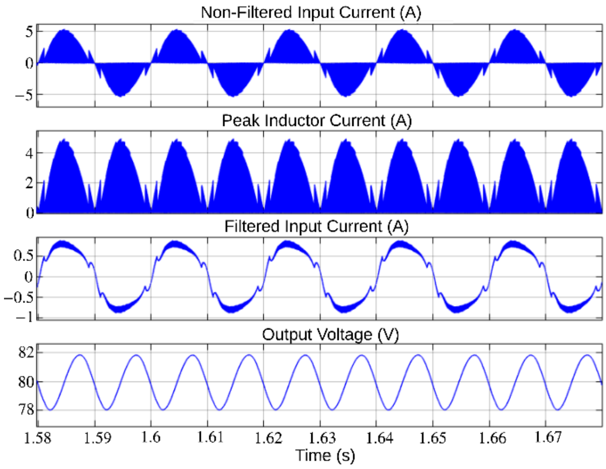

(a)

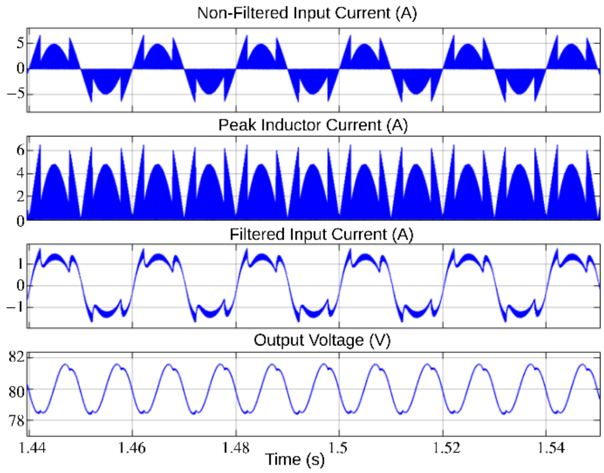

(b)

Figure 13. Input current waveform of the digital COT controlled buck/buck-boost converter (a) for 220V_{AC} input voltage condition (b) for 110V_{AC} input voltage condition (Dijital COT kontrollü düşürücü/düşürücü-yükseltici dönüştürücünün giriş akım formu (a) 220V_{AC} giriş gerilimi koşulu için (b) 110V_{AC} giriş gerilimi koşulu için)

For the COT control method, the simulation reveals a PF of 0.98 and a THD value of 14.69% for the 220V_{AC} *input voltage condition* as shown in Figure 14 (a). Similarly, for the 110 V_{AC} *input voltage condition*, the power factor is measured as 0.94 with a THD value of 33.26% as shown in Figure 14 (b). These results under steady-state conditions indicate the performance of the COT control method.

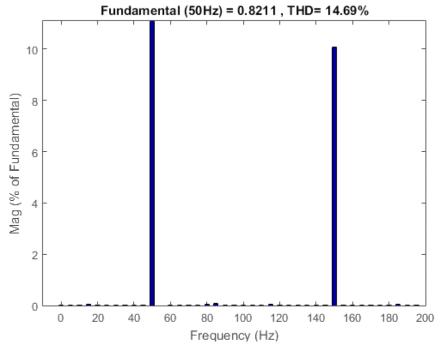

(a)

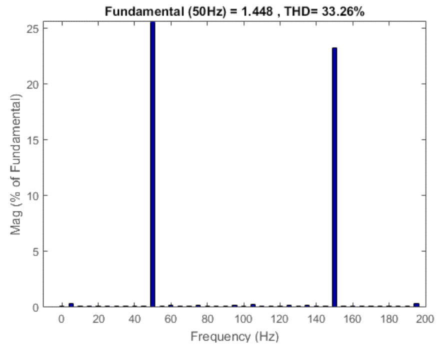

(b)

Figure 14. Input current THD values of digital COT controlled buck/buck-boost converter (a) for 220V_{AC} input voltage condition (b) for 110V_{AC} input voltage condition (Dijital COT kontrollü düşürücü/düşürücü-yükseltici dönüştürücünün giriş akım THD değerleri (a) 220V_{AC} giriş gerilimi koşulu için (b) 110V_{AC} giriş gerilimi koşulu için)

The international current harmonic standard IEC 61000-3-2 applies to equipment using a voltage not less than 220V_{AC} and up to (including) 16 A per phase to limit the emission of harmonic current. Also, IEEE 519 STD standard defines the voltage and current harmonic criteria of the electrical devices. According to this standard, for voltages between 120V-69 kV and currents less than 20 A, the THD of the average current is required to be less than 5%. Therefore, these THD results do not meet either standard.

Moreover, Figure 15 (a) shows the control scheme of the digital VOT controlled buck/buck-boost converter in Matlab/Simulink. Also, Figure 15 (b) shows the digital VOT controller design. It can be seen from the figure that this VOT control scheme is more complex than conventional COT control technique. It should be noted that in both methods, a separate PI controller is designed for the switching elements. Also, unlike the other method, two small resistors (0.125Ω) are placed at the source pin of the switches to measure the current passing through the switches.

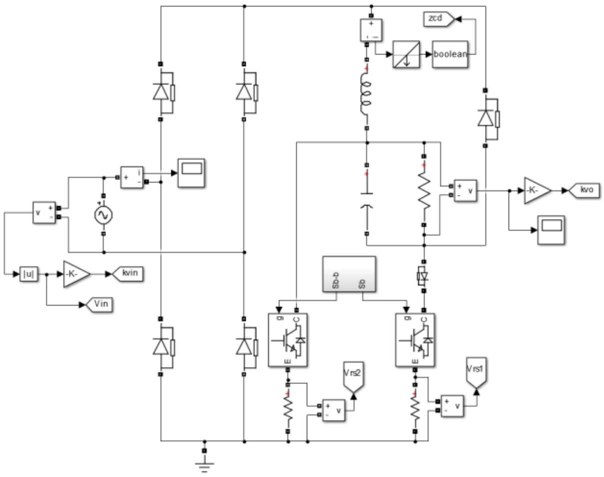

(a)

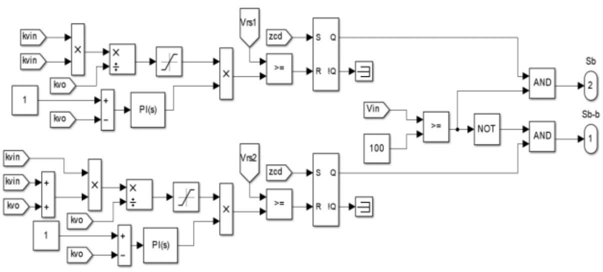

(b)

Figure 15. (a) Control scheme of the digital VOT controlled converter (b) controller design ((a) Dijital VOT kontrollü dönüştürücünün kontrol şeması (b) kontrolör dizaynı)

Figure 16 (a) and (b) show the input current, inductor current, filtered input current and output voltage waveforms of the digital VOT controlled buck/buck-boost converter for 220V_{AC} and 110V_{AC} input voltage scenarios, respectively. As can be seen from the figure, the input current, output voltage and inductor current qualities are better than COT control method.

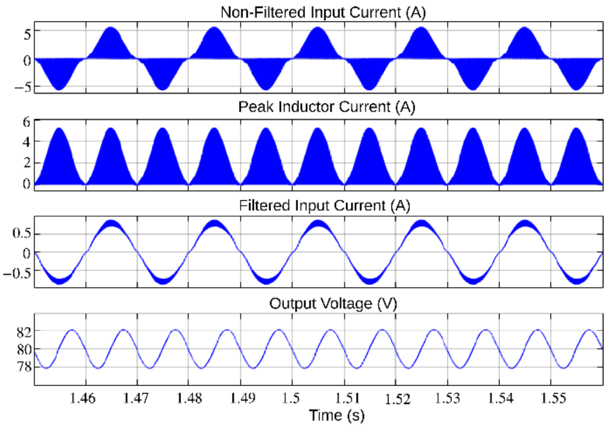

(a)

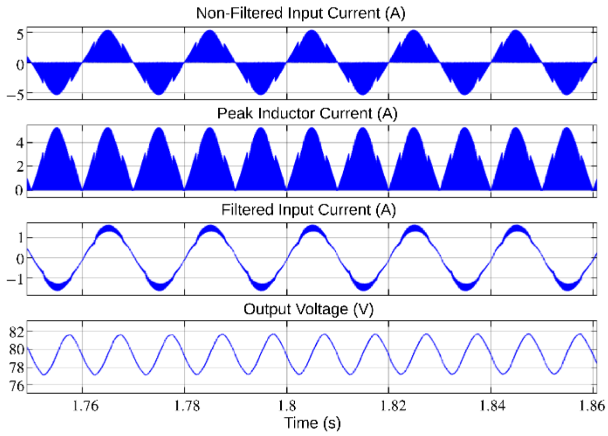

(b)

Figure 16. Input current waveform of the digital VOT controlled buck/buck-boost converter (a) for 220V_{AC} input voltage condition (b) for 110V_{AC} input voltage condition (Dijital VOT kontrollü düşürücü/düşürücü-yükseltici dönüştürücünün giriş akım formu (a) 220V_{AC} giriş gerilimi koşulu için (b) 110V_{AC} giriş gerilimi koşulu için)

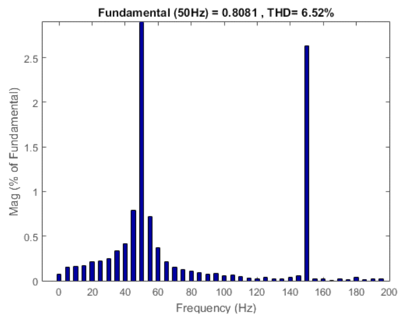

(a)

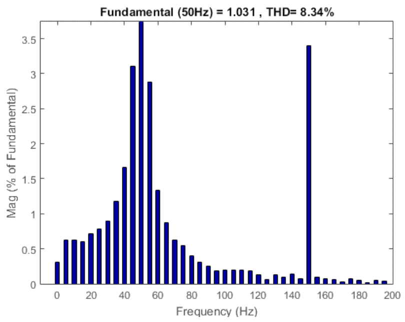

(b)

Figure 17. Input current THD values of the digital VOT controlled buck/buck-boost converter (a) for 220V$_{AC}$ input voltage condition (b) for 110V$_{AC}$ input voltage condition (Dijital VOT kontrollü düşürücü/düşürücü-yükseltici dönüştürücünün giriş akım THD değerleri (a) 220V$_{AC}$ giriş gerilimi koşulu için (b) 110V$_{AC}$ giriş gerilimi koşulu için)

On the other hand, THD simulations using the VOT control method demonstrate superior performance compared to COT. For the 220V$_{AC}$ input voltage condition, the VOT control method achieved a higher PF of 0.99 and a lower THD value of 6.52% as shown in Figure 17 (a). Similarly, for the 110V$_{AC}$ case, the VOT control method exhibited a PF of 0.99 and a THD value of 8.34% as shown in Figure 17 (b). These results highlight the effectiveness of the VOT control method in improving PF and reducing harmonic distortion even if it does not meet the IEEE 519 STD standards. Based on these simulation results, the VOT control method outperforms the COT control method in terms of PF and THD under full load conditions for both 220V$_{AC}$ and 110V$_{AC}$. These findings indicate the potential advantages of using VOT control in AC-DC PFC converters, providing better efficiency and improved performance in terms of power quality.

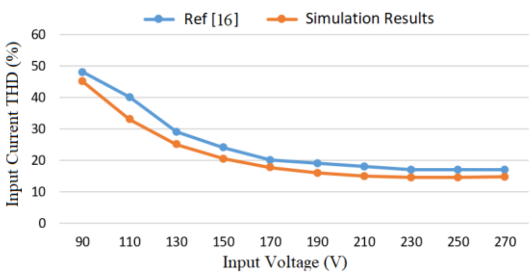

(a)

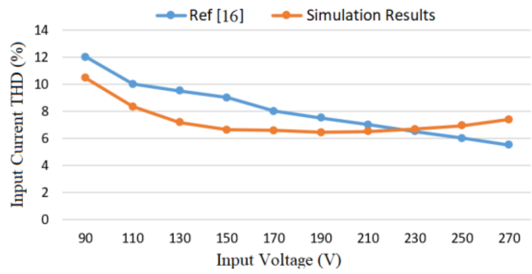

(b)

Figure 18. Input current THD comparison of the topology (a) COT control method (b) VOT control method (Topolojinin giriş gerilim THD karşılaştırması (a) COT kontrol metodu (b) VOT kontrol metodu)

Figure 18 (a) depicts input current THD comparison of the topology with [16] for COT control technique. As can be seen from the figure, data obtained from the simulation studies are compatible with [16]. Also, Figure 18 (b) depicts input current THD comparison of the topology with [16] for VOT control technique. Although it is observed in [16] that THD decreased as the voltage increased, it is observed in this study that THD decreased to a certain level and then increased for VOT control method.

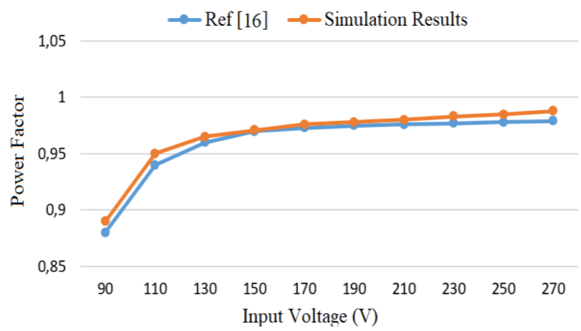

(a)

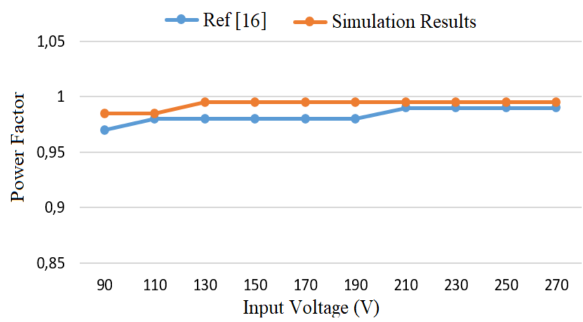

(b)

Figure 19. PF comparison of the topology (a) COT control method (b) VOT control method (Topolojinin PF karşılaştırması (a) COT kontrol metodu (b) VOT kontrol metodu)

Table 2. Calculated and measured parameters of the COT and VOT control methods (COT ve VOT kontrol metodlarının hesaplanan ve ölçülen parametreleri)

Parameters	**COT**				**VOT**			
	$110V_{AC}$		**$220V_{AC}$**		**$110V_{AC}$**		**$220V_{AC}$**	
	Calculated	Measured	Calculated	Measured	Calculated	Measured	Calculated	Measured
PF	0.95 %	0.95 %	0.98 %	0.98 %	1.00 %	0.98 %	1.00 %	0.99 %
THD	32.45 %	33.26 %	14.21 %	14.69 %	7.95 %	8.34 %	6.17 %	6.52 %
$V_{o_{ripple}}$	3.45V	3.50V	3.74V	3.85V	4.10V	4.15V	4.10V	4.17V
$I_{L_{peak}}$	5.8A	5.9A	4.6A	4.8A	5.0A	5.3A	5.0A	5.4A

Figure 19 (a) gives the PF comparison of the topology with [16] for COT control method. Also, Figure 19 (b) gives the PF comparison of the topology with [16] for VOT control method. According to the figure, data obtained from both simulation studies are compatible with [16]. Finally, calculated and measured parameters of the implemented methods are listed in Table 3. According to the table, calculated and measured parameters are compatible with each other.

6. CONCLUSION (SONUÇ)

In this study, a comparative analysis of two control techniques, COT and VOT, for fully digitally controlled CRM buck/buck-boost converter is implemented. The objective is to evaluate and compare the performance of these control strategies in terms of THD and PF.

The results obtained from the simulations performed in the Matlab/Simulink software platform revealed that the VOT control technique outperforms the COT control technique in terms of THD and PF under steady-state conditions. The VOT control method demonstrated higher PF values and lower THD compared to the COT control approach for both $220V_{AC}$ and $110V_{AC}$ input voltage under full load conditions.

The results of this paper ensure valuable insights into strengths and limitations of each control technique. The VOT control strategy offers the advantage of dynamic adaptation of the on-time period based on input and output voltage conditions, resulting in improved load regulation and stability. These benefits make it a suitable choice for AC-DC PFC converters in applications that require high PF and low THD.

DECLARATION OF ETHICAL STANDARDS (ETİK STANDARTLARIN BEYANI)

The author of this article declares that the materials and methods in his work do not require ethical committee approval and/or legal-specific permission.

Bu makalenin yazarı, çalışmasındaki materyal ve yöntemlerin etik kurul onayı ve/veya yasal izin gerektirmediğini beyan eder.

AUTHORS' CONTRIBUTIONS (YAZARLARIN KATKILARI)

***Zafer ORTATEPE*:** He conducted the research, analyzed the results and performed the writing process.

Araştırmayı yapmış, sonuçlarını analiz etmiş ve maklenin yazım işlemini gerçekleştirmiştir.

CONFLICT OF INTEREST (ÇIKAR ÇATIŞMASI)

There is no conflict of interest in this study.

Bu çalışmada herhangi bir çıkar çatışması yoktur.

REFERENCES (KAYNAKLAR)

[1] Baek J, Kim JK, Lee JB, Park MH, Moon GW. A New Standby Structure Integrated with Boost PFC Converter for Server Power Supply. IEEE Trans Power Electron. 2019; 34(6): 5283–5293.
[2] Zhao B, Abramovitz A, Smedley K. Family of Bridgeless Buck-Boost PFC Rectifiers. IEEE Trans Power Electron. 2015; 30(12): 6524–6527.
[3] Yang HT, Chiang HW, Chen CY. Implementation of Bridgeless Cuk Power Factor Corrector With Positive Output

Voltage. IEEE Trans Ind Appl. 2015; 51(4): 3325–3333.
[4] Mahdavi M, Farzanehfard H. Bridgeless SEPIC PFC rectifier with reduced components and conduction losses. IEEE Transactions on Industrial Electronics. 2011; 58(9): 4153–4160.
[5] Yang J, Wu X, Zhang J, Qian Z. Design considerations of a high efficiency ZVS buck AC-DC converter with constant on-time control. International Telecommunications Energy Conference (Proceedings). 2010.
[6] Yang J, Wu X, Zhang J, Qian Z. Variable on-time controlled ZVS buck PFC converter for HB-LED application. Conference Proceedings - IEEE Applied Power Electronics Conference and Exposition - APEC. 2011.
[7] Wu X, Yang J, Zhang J, Xu M. Design considerations of soft-switched buck PFC converter with constant on-time (COT) control. IEEE Trans Power Electron. 2011; 26(11): 3144–3152.
[8] Xie X, Zhao C, Zheng L, Liu S. An improved buck PFC converter with high power factor. IEEE Trans Power Electron. 2013; 28(5): 2277–2284.
[9] Yan T, Xu J, Zhang F, Sha J, Dong Z. Variable-on-time-controlled critical-conduction-mode flyback PFC converter. IEEE Transactions on Industrial Electronics. 2014; 61(11): 6091–6099.
[10] Wu H, Zhang Y, Zhao M, Shen H, Wu X. A constant-on-time based buck controller with active PFC for universal input LED system. Proceedings of the International Conference on Power Electronics and Drive Systems. 2015.
[11] Divya Prabha M V., Seema PN. A novel topology of forward-flyback PFC converter with constant on-time control. Proceedings of IEEE International Conference on Technological Advancements in Power and Energy, TAP Energy. 2015.
[12] Wang X, Yao K, Zhang J. Reducing the switching frequency variation range for CRM buck PFC converter by variable on-time control. Conference Proceedings - IEEE Applied Power Electronics Conference and Exposition - APEC. 2016.
[13] Zhao C, Zhang J, Wu X. An improved variable on-time control strategy for a CRM flyback PFC converter. IEEE Trans Power Electron. 2017; 32(2): 915–919.
[14] Memon AH, Yao K, Chen Q, Guo J, Hu W. Variable-On-Time Control to Achieve High Input Power Factor for a CRM-Integrated Buck-Flyback PFC Converter. IEEE Trans Power Electron. 2017; 32(7): 5312–5322.
[15] Lin HC, Chu WM, Tsai CH, Su WC. A digitally variable on-time controlled PFC flyback converter with primary-side regulation. Proceedings - 7th International Symposium on Next-Generation Electronics. 2018.
[16] Memon AH, Baloach MH, Sahito AA, Soomro AM, Memon ZA. Achieving High Input PF for CRM Buck-Buck/Boost PFC Converter. IEEE Access. 2018; 6: 79082–79093.
[17] Chen J, Yao K, Fang B, Li L, Guan C, Wu C, et al. Segmented Constant-On-Time Control Method for CRM Buck-Buck/Boost PFC Converter. 2019 IEEE Energy Conversion Congress and Exposition (ECCE). 2019.
[18] Yao K, Tang H, Ma C, Wu C. Constant Switching Frequency Control for CRM Buck PFC Converter. IEEE J Emerg Sel Top Power Electron. 2020; 8(4): 4223–4234.
[19] Yao K, Wu C, Chen J, Yang J, Li J, Jin Z, et al. A Scheme to Improve Power Factor and Dynamic Response Performance for CRM/DCM Buck-Buck/Boost PFC Converter. IEEE Trans Power Electron. 2021; 36(2): 1828–1843.
[20] Liu X, Wan Y, He M, Zhou Q, Meng X. Buck-Type Single-Switch Integrated PFC Converter with Low Total Harmonic Distortion. IEEE Transactions on Industrial Electronics. 2021; 68(8): 6859–6870.
[21] Sahlabadi F, Yazdani MR, Faiz J, Adib E. Resonant Bridgeless Buck PFC Converter With Reduced Components and Dead Angle Elimination. IEEE Trans Power Electron. 2022; 37(8): 9515–9523.
[22] Khalili R, Adib E. Soft-Switching Bridgeless Buck PFC With Low THD. IEEE Transactions on Industrial Electronics. 2023; 70(12): 12211–12218.